

this magnitude. Storm total precipitation amounts (in inches) at Salt Lake City, Cedar City, and Flagstaff were 0.05, 0.01, and a trace, respectively. Why did such an impressive trough produce such light precipitation?

The answer can be found by considering the vertical motion field at more levels than 500 mb. Figure 4 shows PIVA for three layers: (a) 700 mb vorticity advected by the 850-500 mb thermal wind (lower level), (b) 500 mb vorticity advected by the 700-300 mb thermal wind (mid level), and (c) 300 mb vorticity advected by the 500-200 mb thermal wind (upper level). Note that in the figures, the advection of vorticity by the thermal wind (right-hand side of equation 1) has actually been calculated. These calculations were performed with software developed at WSFO Salt Lake City based on the NMC mandatory level plot files using a Barnes analysis scheme (Barnes, 1964).

In Figs. 4b and 4c, the upward vertical velocity was at a maximum over northwest Arizona at both the mid and upper levels, respectively. But, in Fig. 4a, the low-level upward vertical velocity was at a maximum to the north over the Nevada-Utah border. (Vertical velocity associated with the actual front is not represented by PIVA because deformation terms have been neglected in the derivation of equation (1). PIVA represents synoptic scale vertical velocity only). In fact, all of Arizona was experiencing low-level subsidence. Figure 5 is the initial LFM relative humidity panel at this time showing moisture to be maximum over central and northeast Nevada. (The NGM and AVN were similar). Thus, the strongest mid- and upper-level lift over northern Arizona was over an area of lower level subsidence, and therefore could not efficiently tap into a low-level source of moisture. To the north over the Nevada-Utah border where lower level lift and moisture were present, mid- and upper-level lift were weak.

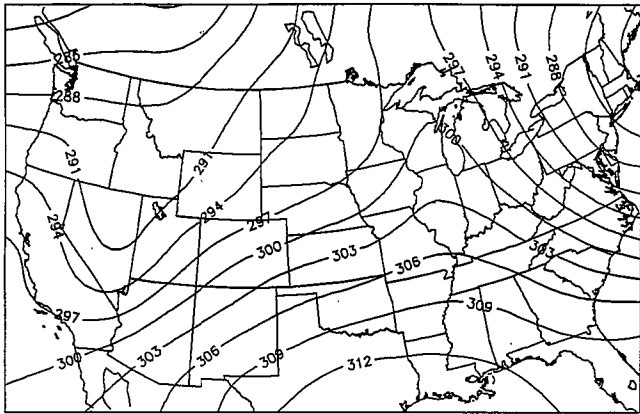
This system that originally appeared to have the necessary ingredients for a major winter storm over the Great Basin was in fact hampered by a discontinuous vertical velocity field. The strong mid- and upper-level synoptic scale lift associated with the trough had dug too far to the south of the lower level synoptic scale lift and moisture. This was not apparent with 500 mb PVA alone. However, by considering a multi-level approach to the vertical motion field, PIVA showed a discontinuous vertical velocity profile. With the coming of AWIPS and gridded data to the field, a multi-level approach in diagnosing synoptic scale vertical motion will likely become routine.

This Technical Attachment is part of a larger COMET project with Prof. Lance Bosart (State University of New York, Albany) investigating Nevada cyclogenesis and its associated frontal structure.

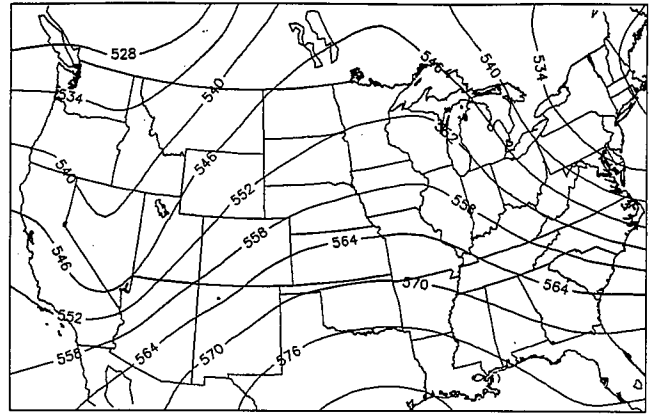
References

- Barnes, S.L., 1964: A technique for maximizing detail in numerical weather map analysis. *J. Appl. Meteor.*, 3, 396-409.
- Chastin, P., 1991: *Graphical Guidance*. 6th ed., National Weather Service Training Center, 166 pp.
- Durran, D.R., and L.W. Snellman, 1987: The diagnosis of synoptic scale vertical motion in an operational environment. *Mon. Wea. Rev.*, 106, 17-31.
- Holton, J.R., 1979: *An Introduction to Dynamic Meteorology*. 2nd ed., Academic Press, 391 pp.
- Trenberth, K.E., 1978: On the interpretation of the diagnostic quasi-geostrophic omega equation. *Mon. Wea. Rev.*, 106, 131-137.
- Western Region Technical Attachment No. 91-48, December 10, 1991.

700 MB HEIGHT MAR 11 1991 12Z



500 MB HEIGHT MAR 11 1991 12Z



300 MB HEIGHT MAR 11 1991 12Z

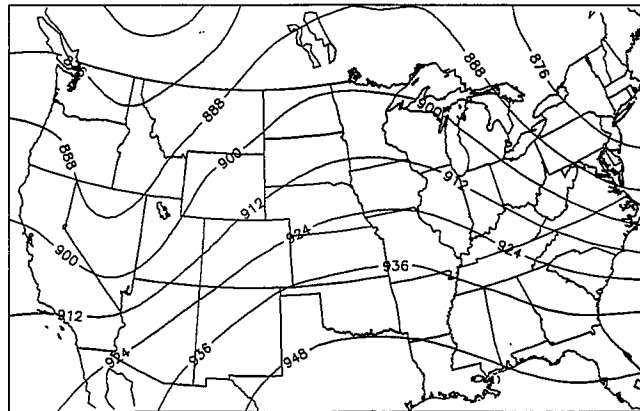


Fig. 1: Geopotential height (decameters) March 11, 1991 1200 UTC at (a) 700 mb, (b) 500 mb, and (c) 300 mb.

300 MB HEIGHT MAR 11 1991 12Z

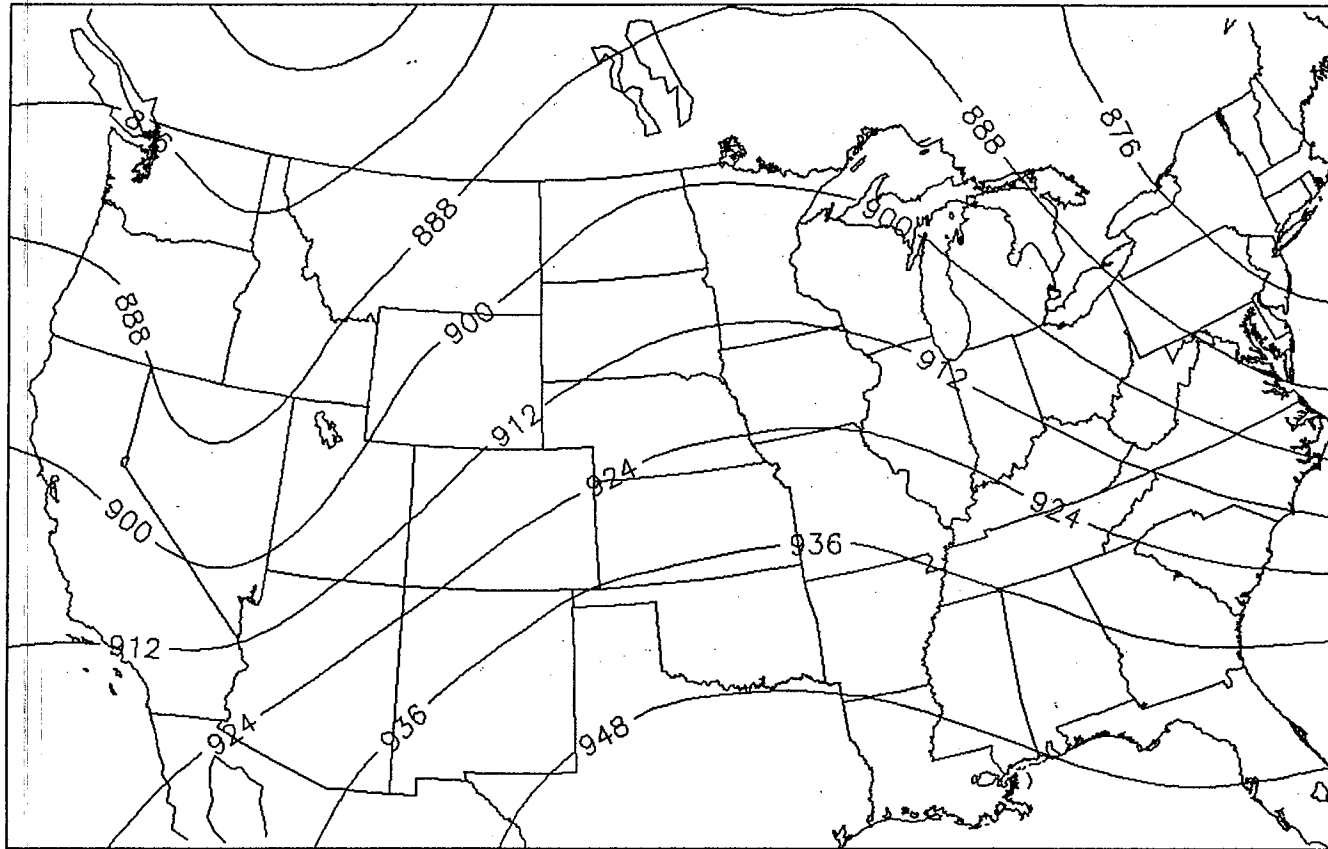
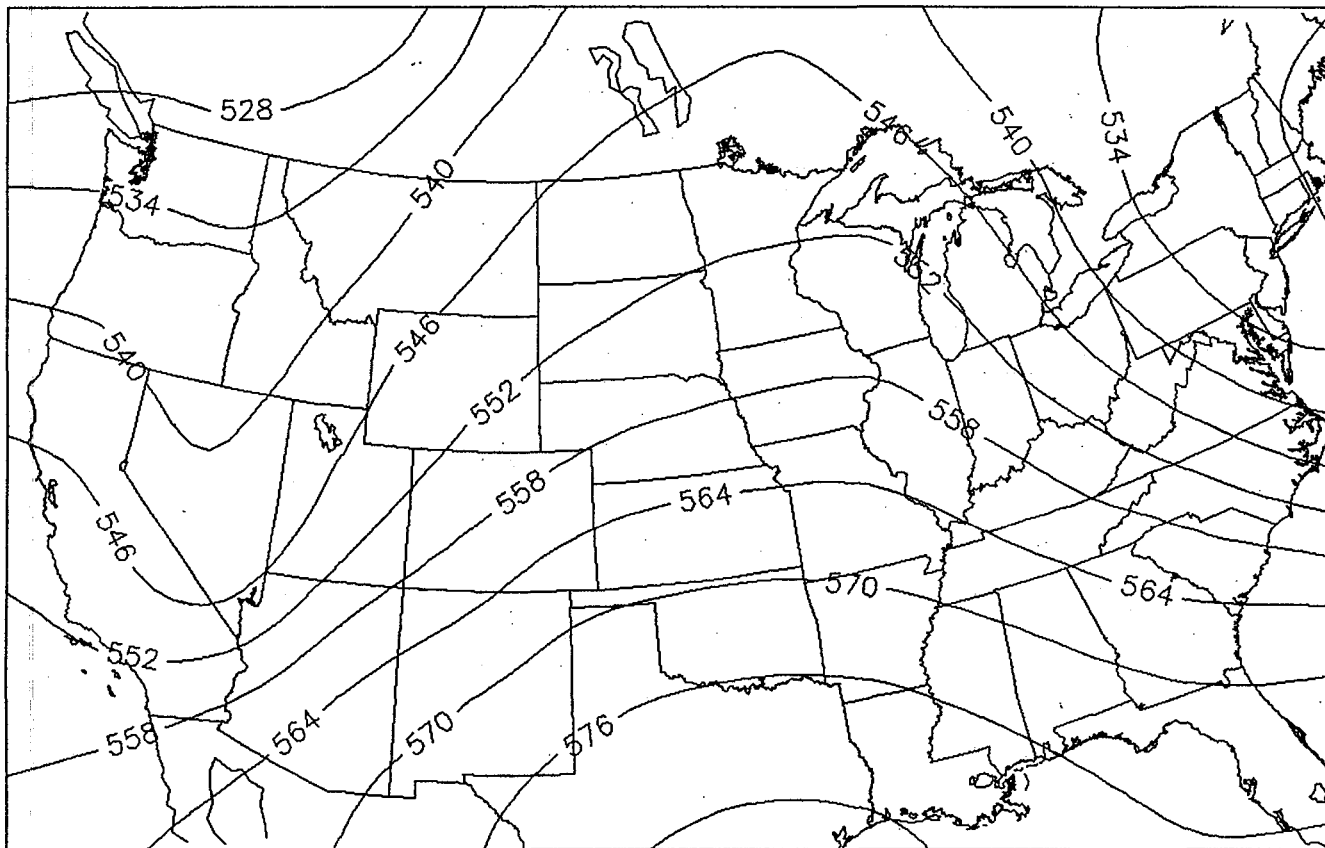
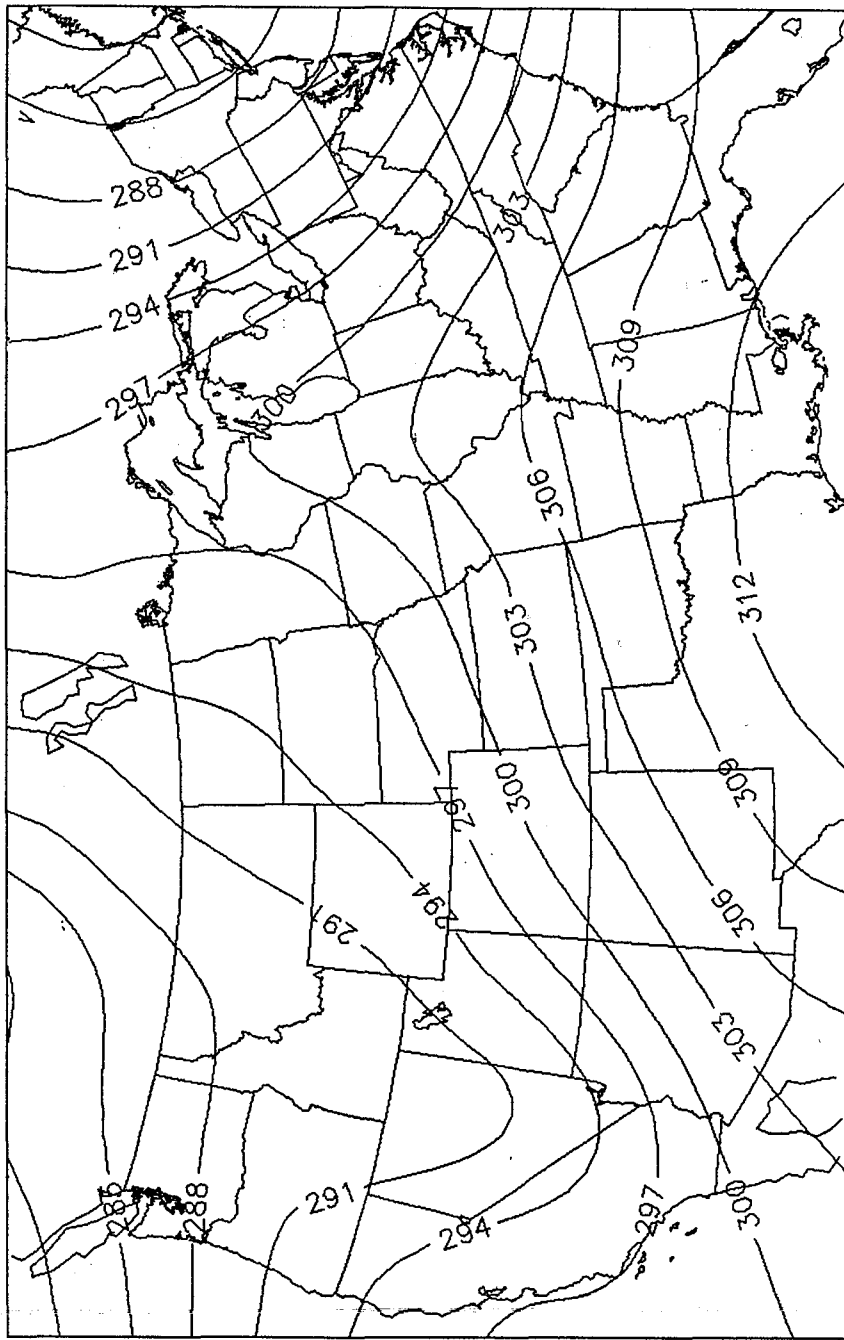


Fig. 1: Geopotential height (decameters) March 11, 1991 1200 UTC at (a) 700 mb, (b) 500 mb, and (c) 300 mb.

500 MB HEIGHT MAR 11 1991 12Z



700 MB HEIGHT MAR 11 1991 12Z



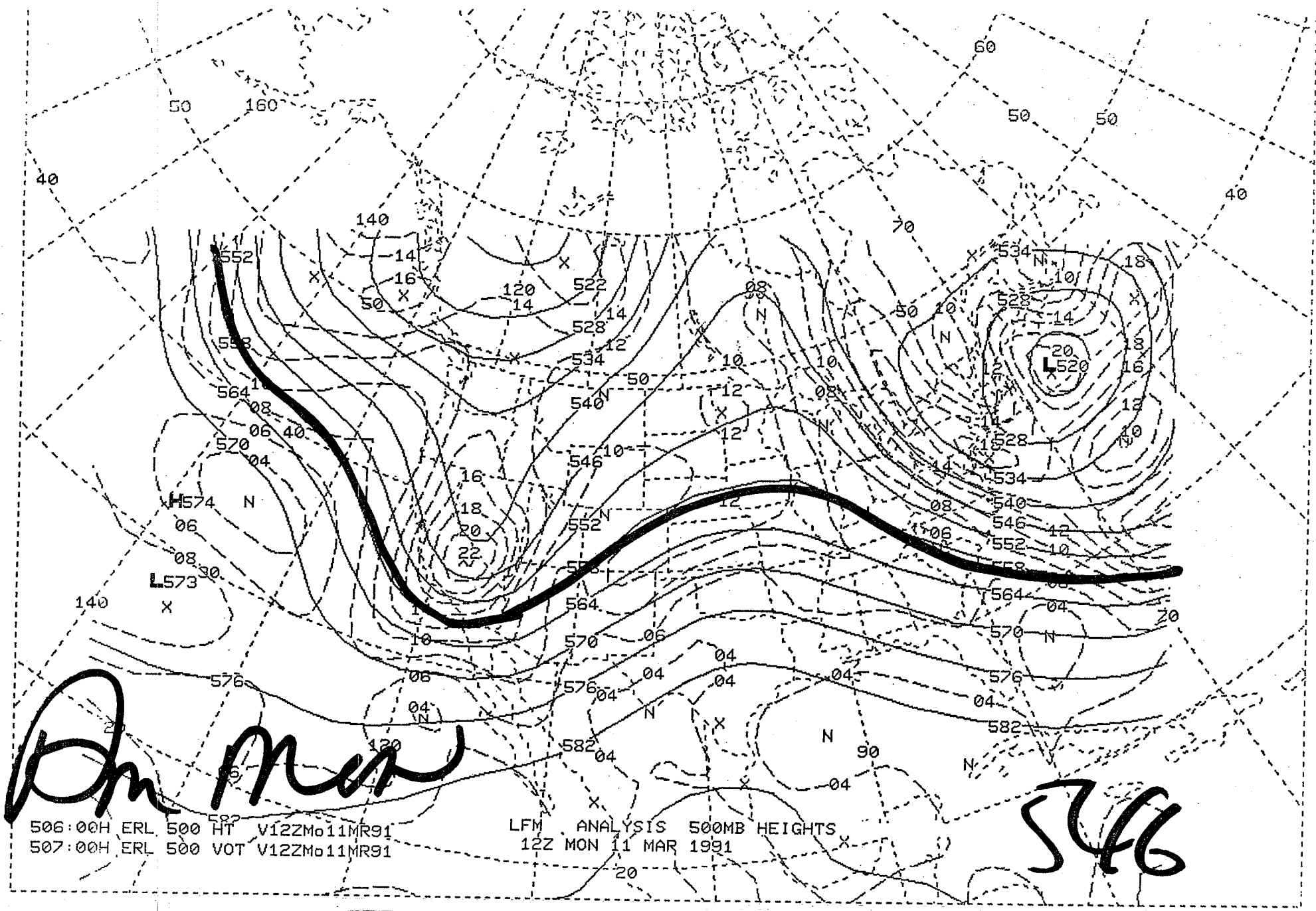


Fig. 2: Initial LFM 500 mb geopotential height and vorticity March 11, 1991 1200 UTC.

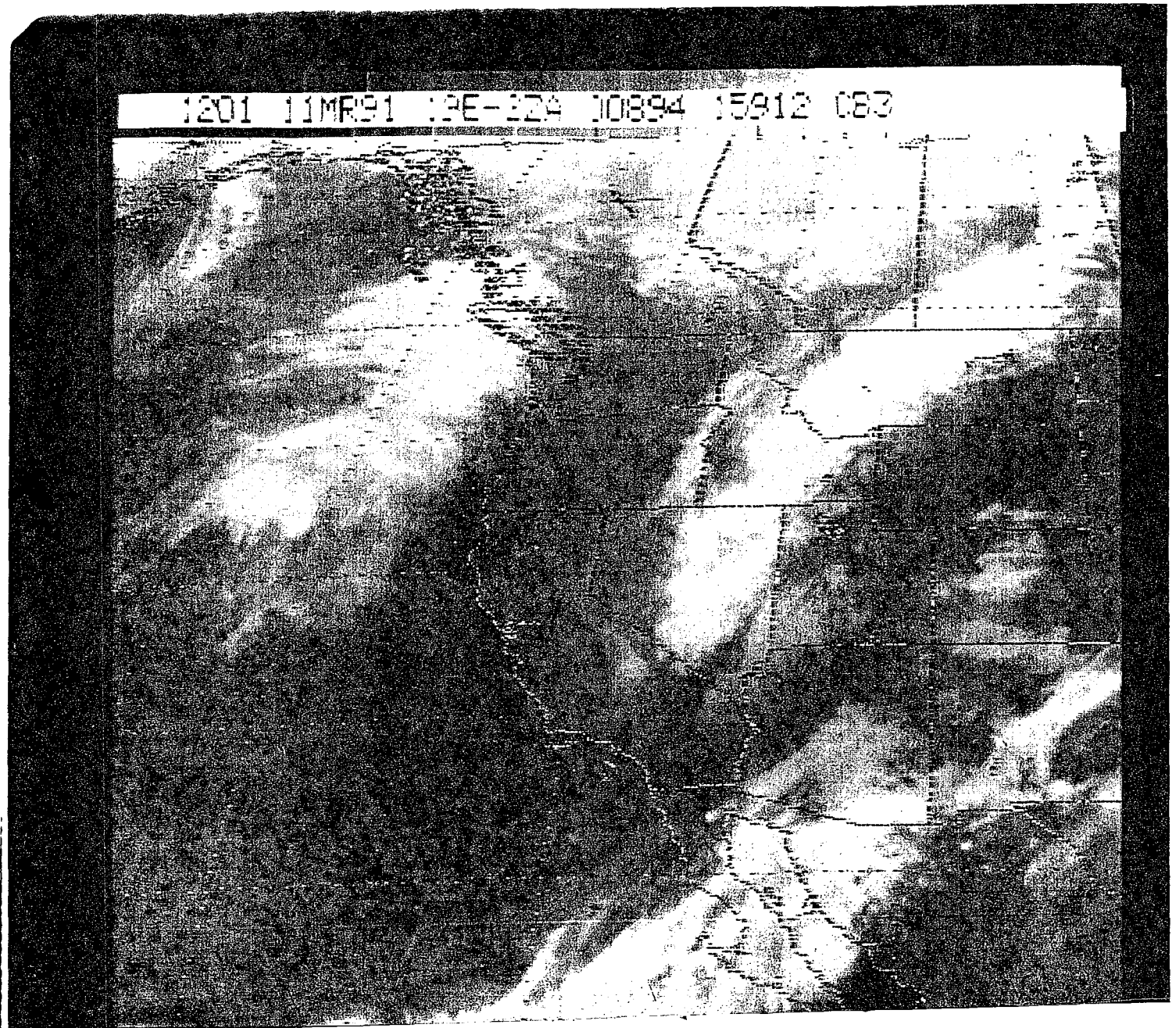


Fig. 3: Infrared satellite picture March 11, 1991 1201 UTC.

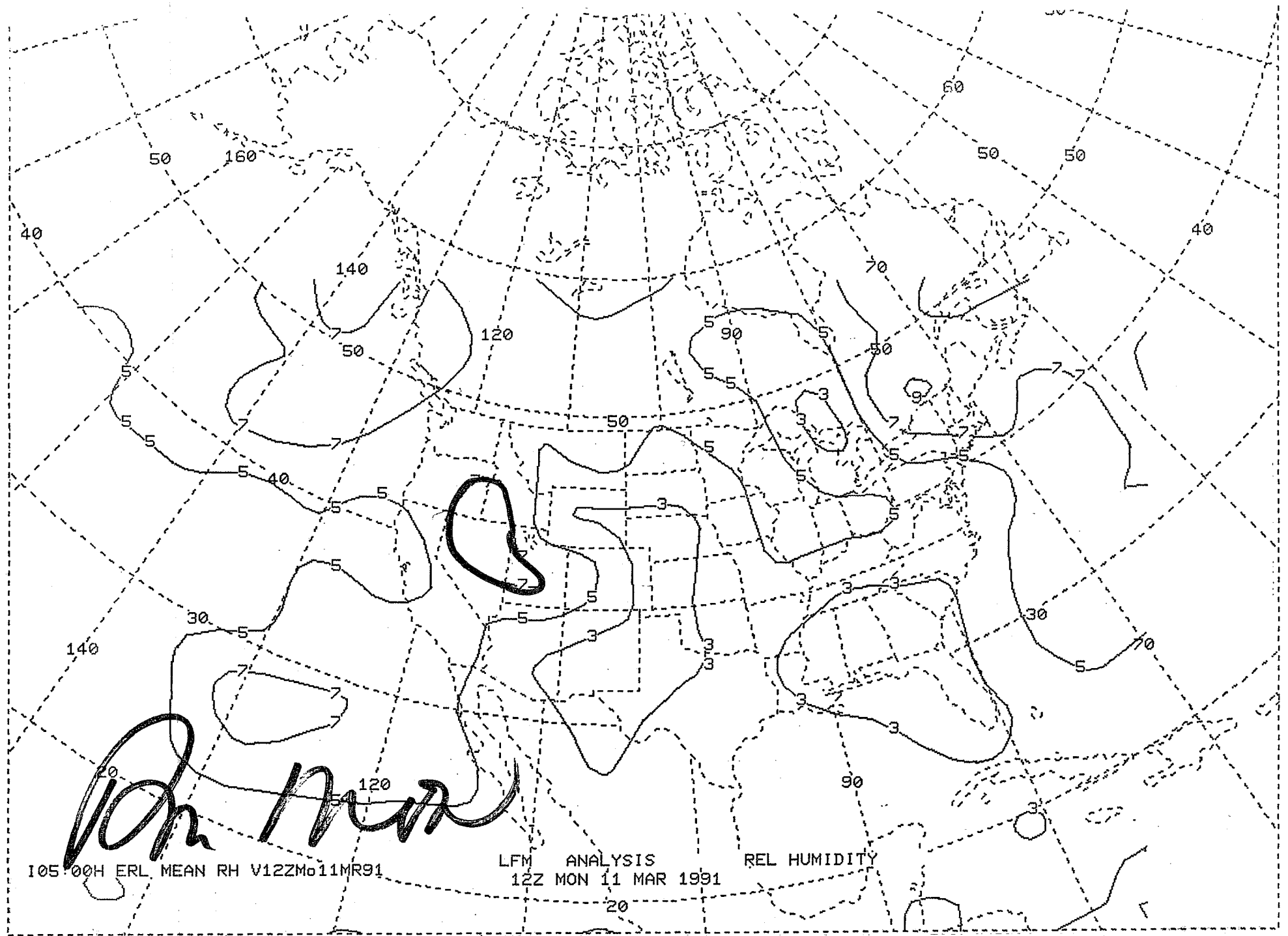


Fig. 5: Initial LFM relative humidity March 11, 1991 1200 UTC.